

Previously, large randomized controlled trials identified several pretreatment factors associated with the final virological outcome, such as genotype, HCV RNA level, degree of fibrosis, age, body weight, ethnicity, and steatosis (25). However, these findings lead us to believe that predicting the final virological response before initiating PEG-IFN alpha and ribavirin is difficult. Indeed, only age and platelet count were associated with the outcome in our patients with genotype 1b and a high viral load. Currently, the final response can be gauged only after treatment has been initiated. Although an early viral response at 12 weeks suggests the eventual outcome with 60–90% accuracy (26), a 12-week regimen is associated with side effects and is expensive. Therefore, this study investigated the baseline expression of genes involving innate immunity that may have significant effects on clinical outcomes.

In the present study, we demonstrated that RIG-I and MDA5 were inducible upon HCV infection, and expression of these intrahepatic positive viral sensors was upregulated in NVR. In vitro studies have suggested that RIG-I and MDA5 play a pivotal role in the regulation of IFN production and augment the production of IFN via an amplification circuit. These results suggest that expression of RIG-I and MDA5 and related amplification system may be up-regulated by endogenous IFN at a higher baseline level in NVR patients. However, HCV elimination by subsequent exogenous IFN is insufficient in these patients, suggesting that NVR patients may have adopted a different equilibrium in their immune response to the virus. In contrast to the expression of RIG-I and MDA5, Cardif mRNA, which was expressed in a relatively constitutive fashion, was significantly lower in NVR. Our ROC analysis highlights lower expression of Cardif

relative to that of RIG-I was one of the strongest predictor for NVR. Moreover, Western blot analysis further confirmed the down regulation of Cardif in NVR patients, as demonstrated by its protein level. Because Cardif is one of the substantial target molecules of HCV evasion (12, 21), it is likely that Cardif expression is suppressed by HCV with resistant phenotype, or is inadequate in NVR patients. Loo et al. have demonstrated a Cardif cleavage product in two of four liver tissue samples of chronic HCV infection (24). In our study, however, the Cardif cleavage product was not detected, presumably because the product could be unstable in vivo, resulting in rapid degradation. Although further studies are necessary to elucidate mechanisms of Cardif down-regulation, our findings of lower expression of Cardif in NVR suggested that the status of Cardif expression in the liver might have a significant effect on the ultimate outcome of antiviral treatment.

The anti-viral effect brought by RIG-I/Cardif signaling is regulated by the coordination of negative and positive regulators. It has been shown that RNF125 functions as a negative regulator of RIG-I/Cardif signaling. RNF125 is an ubiquitin E3-ligase with activity against protein containing CARD domains, such as RIG-I, MDA5, and Cardif, and these ubiquitinated molecules undergo proteasomal degradation. In contrast, RNF125 do not have negative function against LGP2, a negative regulator of RIG-I signaling, because LGP2 lacks CARD domain. In contrast to RIG-I, RNF125 expression was rapidly suppressed by exogenous IFN, therefore, observed lower basal hepatic level of RNF125 in NVR could be explained by suppressive effect of endogenous IFN, which may be up-regulated in NVR patients. Hence, RNF125 may constitute a negative regulatory circuit for IFN production and is responsible for responsiveness to PEG-IFN

and ribavirin therapy.

It has been shown that RIG-I function is modified by ISG15 via ISGylation (18).

Consistent with our data, Chen et al. identified 18 genes, including ISG15 and USP18, whose expression differed between responders and non-responders (27). Interestingly, a recent study has shown that USP18 negatively regulates IFN signaling independently of its isopeptidase activity towards ISG15 by binding to the IFNAR2 receptor subunit and blocking the interaction between Janus kinase (JAK) and the IFN receptor (28).

Moreover, the siRNA knockdown of USP18 in human cells has consistently been shown to potentiate the ability of IFN to inhibit HCV RNA replication (29). Therefore, USP18 is suggested as a novel *in vivo* inhibitor of signal transduction pathways that are specifically triggered by type I IFN. Consistent with a role for USP18 in down regulating the antiviral IFN response, we confirmed that up-regulation of USP18 was one of the factors predicting a lack of response to treatment with IFN.

The mechanism underlying the association of gene expression involving innate immunity with resistance to therapy is not well understood. Our human study with HCV patients treated by PEG-IFN and ribavirin highlights RIG-I/Cardif, RIG-I/RNF125, and ISG15/USP18, which is partly responsible for the clinical responsiveness to antiviral therapy. RIG-I signaling by viral pathogens may affect a wide variety of responses in not only innate but also acquired immunity. Our study is the first to demonstrate the potential relevance between molecules involving innate immunity and the clinical response to antiviral therapy.

In addition, sequential analysis of expression profile during PEG-IFN alpha-2b and ribavirin was also performed in this study. Lanford et al. demonstrated transcriptional response to IFN alpha in chimpanzee by genome microarray analysis, which included RIG-I, ISG15, and USP18 (30). An association of transcriptional response with early phase of virological response has been also reported in PBMC or liver biopsy specimen (31-33). We recently reported that the transcriptional double-stranded RNA-activated protein kinase (PKR) response during treatment with PEG-IFN alpha-2b and ribavirin was associated with the ultimate clinical response (31). Similarly, the present study demonstrated a strong and rapid increase of RIG-I, ISG15 and USP18 mRNA in response to clinical PEG-IFN treatment especially in SVR patients, although few patients were available to achieve statistical significance between SVR and NVR. In marked contrast, transcriptional response of RNF125 exhibited a triphasic pattern. Rapid suppression seen in the first phase was presumably because of a negative regulatory effect of IFN. However, increase of RNF125 mRNA in the second phase, which tended to be greater in NVR, may be responsible for inhibiting RIG-I expression seen in 8–48 hours after PEG-IFN alpha-2b administration. Although limitations including the use of PBMC and small sample size still deserve mention, the sequential expression profile during treatment may provide further valuable information regarding the prediction of the clinical response to the therapy and the mechanism of action of antiviral treatment.

In the present study, we have included patients with genotype 1b, because it is imperative to designate a virologically homogenous patient group to associate individual treatment responses with different gene expression profiles that direct innate immune responses. We have preliminarily studied genotype 2 patients and found that Cardiff and

RNF125 gene expression levels in NVR patients were significantly lower than those with SVR patients ($p = 0.03$ and 0.04 , respectively), and that RIG-I/Cardif and RIG-I/RNF125 ratios were significantly higher in NVR patients ($p = 0.02$ and 0.009 , respectively, *see the Supplementary Figure 2*). These findings suggest that the differences in gene expression profiles between SVR and NVR were almost identical to those demonstrated in patients with genotype 1b. However, the correlation between treatment responses in all the genotypes and the different status of innate immune responses needs to be explored. Further studies may be necessary to clarify this issue.

In conclusion, the results of the present study offer potentially important clinical implications for patients with chronic hepatitis C who are treated with PEG-IFN alpha and ribavirin. Quantifying hepatic gene expression of the RIG-I/Cardif system, including its regulators before treatment, is useful in identifying patients who are at a higher risk for NVR. The data from these assays can provide valuable information that may influence the decision about the treatment strategy in each individual patient. Finally, this clinical human study demonstrates the potential relevance of the molecules involving innate immunity to the clinical response to therapy. Our data will help understand the pathogenesis of HCV resistance and development of new antiviral therapy targeted toward the innate immune system.

REFERENCES

1. Kiyosawa K, Sodeyama T, Tanaka E, et al. Interrelationship of blood transfusion, non-A, non-B hepatitis and hepatocellular carcinoma: analysis by detection of antibody to hepatitis C virus. *Hepatology* 1990;12:671-675.
2. Manns MP, McHutchison JG, Gordon SC, et al. Peginterferon alfa-2b plus ribavirin compared with interferon alfa-2b plus ribavirin for initial treatment of chronic hepatitis C: a randomised trial. *Lancet* 2001;358:958-965.
3. Fried MW, Shiffman ML, Reddy KR, et al. Peginterferon alfa-2a plus ribavirin for chronic hepatitis C virus infection. *N Engl J Med* 2002;347:975-982.
4. Hadziyannis SJ, Sette HJ, Morgan TR, et al. PEGASYS International January 2006 American Gastroenterological Association 253 Study Group. Peginterferon-alpha2a and ribavirin combination therapy in chronic hepatitis C: a randomized study of treatment duration and ribavirin dose. *Ann Intern Med* 2004;140:346-355.
5. Zeuzem S, Pawlotsky JM, Lukasiewicz E, et al. DITTO-HCV Study Group. International, multicenter, randomized, controlled study comparing dynamically individualized versus standard treatment in patients with chronic hepatitis C. *J Hepatol* 2005;43:250-257.
6. Berg T, von Wagner M, Nasser S, et al. Extended treatment duration for hepatitis C virus type 1: comparing 48 versus 72 weeks of peginterferon-alfa-2a plus ribavirin. *Gastroenterology* 2006;130:1086-1097.
7. Biron CA. Initial and innate responses to viral infections--pattern setting in immunity or disease. *Curr Opin Microbiol* 1999;2:374-381.

8. Gale M Jr, Foy EM. Evasion of intracellular host defence by hepatitis C virus. *Nature* 2005;436:939-945.
9. Yoneyama M, Kikuchi M, Natsukawa T, et al. The RNA helicase RIG-I has an essential function in double-stranded RNA-induced innate antiviral responses. *Nat Immunol* 2004;5:730-737.
10. Yoneyama M, Kikuchi M, Matsumoto K, et al. Shared and unique functions of the DExD/H-box helicases RIG-I, MDA5, and LGP2 in antiviral innate immunity. *J Immunol* 2005;175:2851-2858.
11. Yoneyama M, Kikuchi M, Matsumoto K, et al. Shared and unique functions of the DExD/H-box helicases RIG-I, MDA5, and LGP2 in antiviral innate immunity. *J Immunol*. 2005;175:2851-2858.
12. Meylan E, Curran J, Hofmann K, et al. Cardif is an adaptor protein in the RIG-I antiviral pathway and is targeted by hepatitis C virus. *Nature* 2005;437:1167-1172.
13. Kawai T, Takahashi K, Sato S, et al. IPS-1, an adaptor triggering RIG-I- and Mda5-mediated type I interferon induction. *Nat Immunol* 2005;6:981-988.
14. Seth RB, Sun L, Ea CK, et al. Identification and characterization of MAVS, a mitochondrial antiviral signaling protein that activates NF-kappaB and IRF 3. *Cell* 2005;122:669-682.
15. Xu LG, Wang YY, Han KJ, et al. VISA is an adapter protein required for virus-triggered IFN-beta signaling. *Mol Cell* 2005;19:727-740.
16. Rothenfusser S, Goutagny N, DiPerna G, et al. The RNA helicase Lgp2 inhibits TLR-independent sensing of viral replication by retinoic acid-inducible gene-I. *J Immunol* 2005;175:5260-5268.

17. Arimoto K, Takahashi H, Hishiki T, et al. Negative regulation of the RIG-I signaling by the ubiquitin ligase RNF125. *Proc Natl Acad Sci USA*. 2007;104:7500-7505.
18. Zhao C, Denison C, Huibregtse JM, et al. Human ISG15 conjugation targets both IFN-induced and constitutively expressed proteins functioning in diverse cellular pathways. *Proc Natl Acad Sci USA*. 2005;102:10200-10205.
19. Schwer H, Liu LQ, Zhou L, et al. Cloning and characterization of a novel human ubiquitin-specific protease, a homologue of murine UBP43 (Usp18). *Genomics* 2000;65:44-52.
20. Malakhov MP, Malakhova OA, Kim KI, et al. UBP43 (USP18) specifically removes ISG15 from conjugated proteins. *J Biol Chem* 2002;277:9976-9981.
21. Li XD, Sun L, Seth RB, et al. Hepatitis C virus protease NS3/4A cleaves mitochondrial antiviral signaling protein off the mitochondria to evade innate immunity. *Proc Natl Acad Sci USA* 2005;102:17717-17722.
22. Nakagawa M, Sakamoto N, Tanabe Y, et al. Suppression of hepatitis C virus replication by cyclosporin A is mediated by blockade of cyclophilins. *Gastroenterology* 2005;129:1031-1041.
23. Asahina Y, Izumi N, Uchihara M, et al. A potent antiviral effect on hepatitis C viral dynamics in serum and peripheral blood mononuclear cells during combination therapy with high-dose daily interferon alpha plus ribavirin and intravenous twice-daily treatment with interferon beta. *Hepatology* 2001;34:377-384.
24. Loo YM, Owen DM, Li K, et al. Viral and therapeutic control of IFN-beta promoter stimulator 1 during hepatitis C virus infection. *Proc Natl Acad Sci USA* 2006;103:6001-6006.

25. Dienstag JL, McHutchison JG. American Gastroenterological Association technical review on the management of hepatitis C. *Gastroenterology* 2006;130:231-264.
26. National Institute of Health. National Institute of Health Consensus Development Statement: management of hepatitis. *Hepatology* 2002;36(Suppl 1):S3-S20.
27. Chen L, Borozan I, Feld J, et al. Hepatic gene expression discriminates responders and nonresponders in treatment of chronic hepatitis C viral infection. *Gastroenterology* 2005;128:1437-1444.
28. Malakhova OA, Kim KI, Luo JK, et al. UBP43 is a novel regulator of interferon signaling independent of its ISG15 isopeptidase activity. *EMBO J* 2006;25:2358-2367.
29. Randall G, Chen L, Panis M, et al. Silencing of USP18 potentiates the antiviral activity of interferon against hepatitis C virus infection. *Gastroenterology* 2006;131:1584-1591.
30. Lanford RE, Guerra B, Lee H, et al. Genomic response to interferon-alpha in chimpanzees: implications of rapid downregulation for hepatitis C kinetics. *Hepatology* 2006;43:961-972.
31. Asahina Y, Izumi N, Umeda N, et al. Pharmacokinetics and enhanced PKR response in patients with chronic hepatitis C treated with pegylated interferon alpha-2b and ribavirin. *J Viral Hepat* 2007;14:396-403.
32. Taylor MW, Tsukahara T, Brodsky L, et al. Changes in gene expression during pegylated interferon and ribavirin therapy of chronic hepatitis C virus distinguish responders from nonresponders to antiviral therapy. *J Virol* 2007;81:3391-3401.

33. Feld JJ, Nanda S, Huang Y, et al. Hepatic gene expression during treatment with peginterferon and ribavirin: Identifying molecular pathways for treatment response. *Hepatology* 2007;46:1548-1563.

FIGURE LEGENDS

Figure 1. Comparison of hepatic gene expression levels between chronic hepatitis C patients (n = 74) and non-viral liver disease patients (n = 5). Expression levels of RIG-I, MDA5, LGP2, Cardif, RNF125, ISG15, and USP18 are shown. Error bars indicate the standard error. Upon HCV infection, expression of these genes except Cardif was stimulated. The p values determined by Mann–Whitney U-test between two groups were as follows: RIG-I, 0.02; MDA5, 0.01; LGP2, 0.005; Cardif, 0.7; RNF125, 0.06; ISG15, 0.007; USP18, 0.004.

Figure 2. Comparison of hepatic gene expression levels according to final virological outcome. Expression levels of RIG-I, MDA5, LGP2, ISG15, USP18, Cardif, RNF125, RIG-I/Cardif ratio and RIG-I/RNF125 ratio are shown. Open column indicates SVR (n = 30), gray column indicates TR (n = 24), and closed column indicates NVR (n = 20). Error bars indicate the standard error. The p values were analyzed by the Kruskal–Wallis test.

Figure 3. Receiver operator characteristic (ROC) curve for prediction of non-virological response. ROC curves were generated to compare (A) RIG-I/Cardif ratio (black line) and RIG-I/RNF125 ratio (gray line), (B) RIG-I (black line), MDA5 (gray line), and LGP2 (dotted line), and (C) ISG15 (black line) and USP18 (gray line).

Figure 4. (A) Western blot analysis. Five were SVR (lanes 1–5), four were NVR (lanes 6–9), and three were non-HCV control (lanes 10–12). Specific bands for Cardif and beta-actin are indicated by arrows. (B) Expression level of Cardif protein

normalized to beta-actin in the liver biopsy specimens according to ultimate treatment response. Error bars indicate the standard error.

Figure 5. Transcriptional responses during PEG-IFN alpha-2b and ribavirin therapy in PBMC (n = 14). Open column indicates SVR (n = 7) and closed column indicates NVR (n = 7). Error bars indicate the standard error. The p values determined by Mann–Whitney U-test between two groups at 8 hours were as follows: RIG-I, 0.3; RNF125, 0.3; Cardif, 0.7; ISG15, 0.3; USP18, 0.2.

Supplementary Figure 1. Host antiviral innate defense system proposed by in vitro experiments. Upon viral infection, cytoplasmic viral sensors (RIG-I and MDA5) detect viral pathogens, resulting in IFN beta gene activation via Cardif, an adaptor molecule. RIG-I/MDA5 sensing is negatively regulated by LGP2, a dominant negative viral sensor lacking CARD. RIG-I, MDA5, and Cardif are ubiquitinated by RNF125, a specific E3-ligase, which results in suppression the functions of these molecules via the ubiquitin-proteasome pathway. Cytoplasmic viral sensors and molecules involving IFN signal transduction (Jak1 and STAT1) are ISGylated by ISG15, a ubiquitin-like protein, and this function is suppressed by USP18, a specific protease that remove ISG15 from ISGylated protein. HCV-NS3/4A specifically cleaves Cardif as part of its immune evasion strategy.

Supplementary Figure 2. Comparison of hepatic gene expression levels between SVR and NVR in patients with genotype 2. Open column indicates SVR (n = 5) and closed column indicates NVR (n = 5). Error bars indicate the standard error. The p values were

analyzed by Mann–Whitney U-test (RIG-I, 0.3; MDA5, 0.1; LGP2, ISG15, 0.03; USP18, 0.6; Cardif, 0.03; RNF125, 0.04; RIG-I/Cardif, 0.02; and RIG-I/RNF125, 0.009).

Table 1. Patient characteristics at baseline according to final virological response

	SVR n = 30	TR n = 24	NVR n = 20	p value
Age (y. o.)	52 ± 13	60 ± 8.7	60 ± 10	0.04*
Female % (M/F)	47% (16/14)	63% (9/15)	60% (8/12)	0.5 [†]
Naïve & Relapser [‡] /Non-responder [‡]	26/4	20/4	14/6	0.3 [‡]
BMI	24.6 ± 3.0	24.9 ± 4.4	24.0 ± 2.1	0.6*
ALT (IU/L)	75 ± 57	65 ± 35	68 ± 41	1.0*
Hemoglobin (g/dL)	14.3 ± 1.6	14.1 ± 1.1	14.5 ± 1.7	0.6*
Platelet count (×10 ³ /μL)	182 ± 62	169 ± 48	140 ± 39	0.04*
Liver histology				
A1/A2/A3	19/8/3	14/8/1	10/10/0	0.3 [‡]
F1/F2/F3	14/9/7	11/7/5	7/5/8	0.7 [‡]
Viral load (×10 ⁶ IU/mL)	1.6 ± 1.2	1.8 ± 1.1	1.6 ± 1.1	0.8*
Viral decline rate (log ₁₀ /day)				
First phase	2.1 ± 0.9	1.5 ± 0.6	0.7 ± 0.5	< 0.0001*
Second phase	0.05 ± 0.05	0.04 ± 0.02	0.006 ± 0.008	< 0.0001*

*The p values were determined by Kruskal–Wallis test.

[†]The p values were determined by chi-square test.

[‡]Response to previous IFN treatment

BMI: body mass index

ALT: alanine aminotransferase

Table 2. Area under the ROC curves, sensitivity, specificity, and negative and positive predictive values of non-virological responses

Variables	Az	95% CI	Cut-off	Sensitivity	Specificity	NPV*	PPV†
RIG-I	0.89	0.78–0.95	0.68	0.80	0.87	0.92	0.70
MDA5	0.92	0.86–0.98	0.84	0.82	0.89	0.93	0.74
LGP2	0.76	0.63–0.90	1.03	0.65	0.72	0.85	0.46
RIG-I/Cardif	0.91	0.84–0.99	0.88	0.75	0.91	0.91	0.75
RIG-I/RNF125	0.81	0.69–0.93	1.05	0.82	0.62	0.91	0.43
ISG15	0.91	0.85–0.97	0.36	0.90	0.81	0.96	0.64
USP18	0.90	0.84–0.96	0.67	0.90	0.83	0.96	0.67

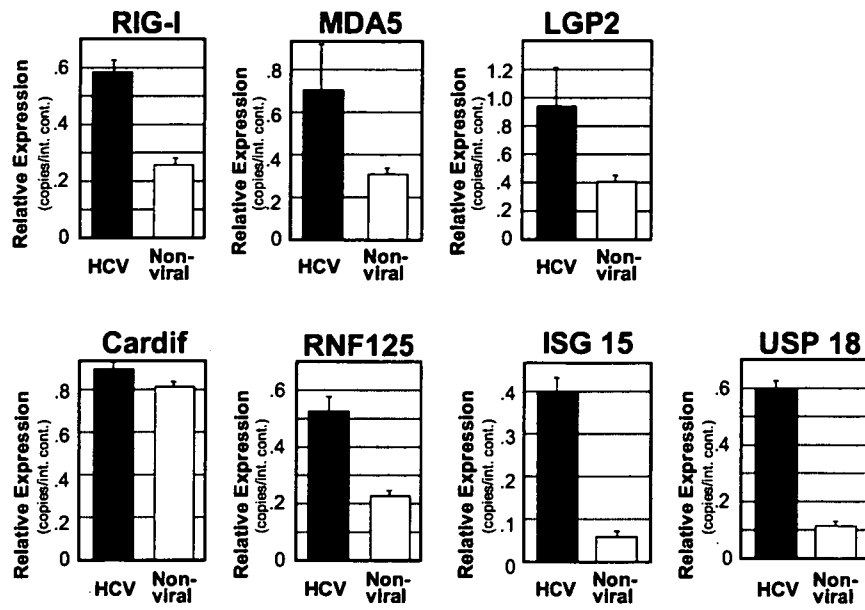
*NPV: negative predictive value

†PPV: positive predictive value

Table 3. Multivariate analysis for the factors associated with non-virological response

Variable	Odds Ratio	95% CI	P value
RIG-I/Cardif Ratio (by 0.1)	1.5	1.1–2.1	0.008
RIG-I/RNF125 Ratio (by 0.1)	1.2	1.0–2.5	0.1
ISG15 (by 0.1/internal control)	1.5	1.1–2.0	0.01
Age (by 1 yr)	1.0	0.9–1.1	0.6
Platelet count (by $1 \times 10^4/\mu\text{L}$)	1.2	0.9–1.5	0.07

Figure 1



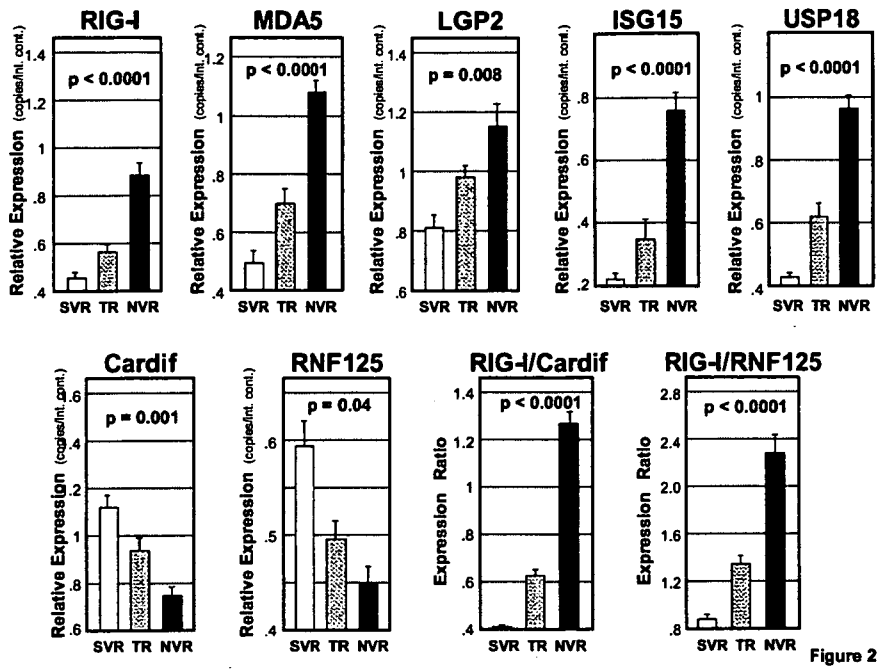


Figure 2

Figure 3

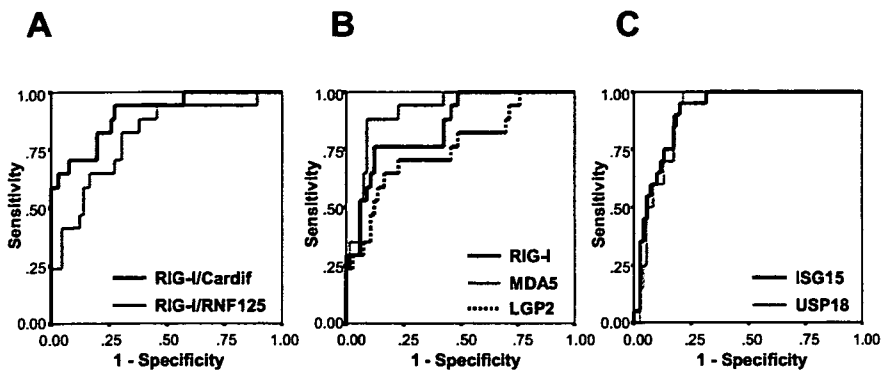


Figure 4

